Soft x-ray electron temperature measurements on Alcator C-Mod

J. Maddox, L. Delgado-Aparicio, N. Pablant, K. Hill, M. Bitter, J. Rice, A. Hubbard

UC Berkeley, Princeton Plasma Physics Laboratory (PPPL)

MIT Plasma Science Fusion Center (PSFC)

Motivation for additional electron temperature diagnostic

The most common electron temperature diagnostics, Thomson Scattering (TS) and Electron Cyclotron Emission (ECE), both require large diagnostic footprints and expensive optics.

Another electron temperature diagnostic is the Pulse-Height-Analysis (PHA) system, which derives the electron temperature from the x-ray bremsstrahlung continuum [1,2]. However, the main disadvantage of the PHA method is poor temporal resolution of the Si(Li) diode detectors [1].

X-ray pinhole camera uses a pixilated Pilatus detector that allows single photon counting at a rate 1MHz per pixel and the setting of energy thresholds [3, 4].

The detector configuration is optimized by Shannon-sampling theory [5], such that spatial profiles of the x-ray continuum intensity can be obtained simultaneously for different energies.

The exponential-like dependence of the x-ray intensity with photon energies is compared with a model describing the Be filter, attenuation in air, and detector efficiency, as well as different sets of energy thresholds [6].

Method for detecting and counting X-Rays and setting different energy thresholds.

The number of X-rays detected from the Dectris photodiode is given by the density and temperature expression below. Where C is a constant n_e is electron density, Z_{eff} is the effective charge of the plasma.

$$I_{x-ray} \propto \frac{C n_e^2 Z_{eff}}{T^{1/2}} \int_0^\infty \frac{exp(-E/T_e)}{E} Tr^{Be} Tr^{Air} Ab^{Si} S_{Detector} dE$$

The transmission terms inside the integral, Tr, can be approximated with an exponential, while the Si absorption is formulated from Tr + Ab = 1 so Ab = 1-Tr.

$$Tr^x \approx exp(E_0^3/E^3) \qquad E_0 = (2N r_0 hc\tau k^2)^{1/3} = (ln2)^{1/3} E_{C,50\%}$$

The E_0 term is formulated based on the thickness and atomic density of the material in addition to an energy scaling factor k [4, 6]. In practice we relate this to the photon energy where the material transmits 50% of the incoming photons, $E_{C,50\%}$ [3. 4].

In addition we account for the electrical response of the detector which is fitted with an error function and an E_0 term used in the transmission calculation [10].

$$S_{Detector} = \frac{1}{2}(1 + erfc(E_0^3/E^3))$$

The detector works by exciting a potential difference across each pixel when it is struck by a photon. If the potential difference is greater than the threshold voltage, the photon is counted [3].

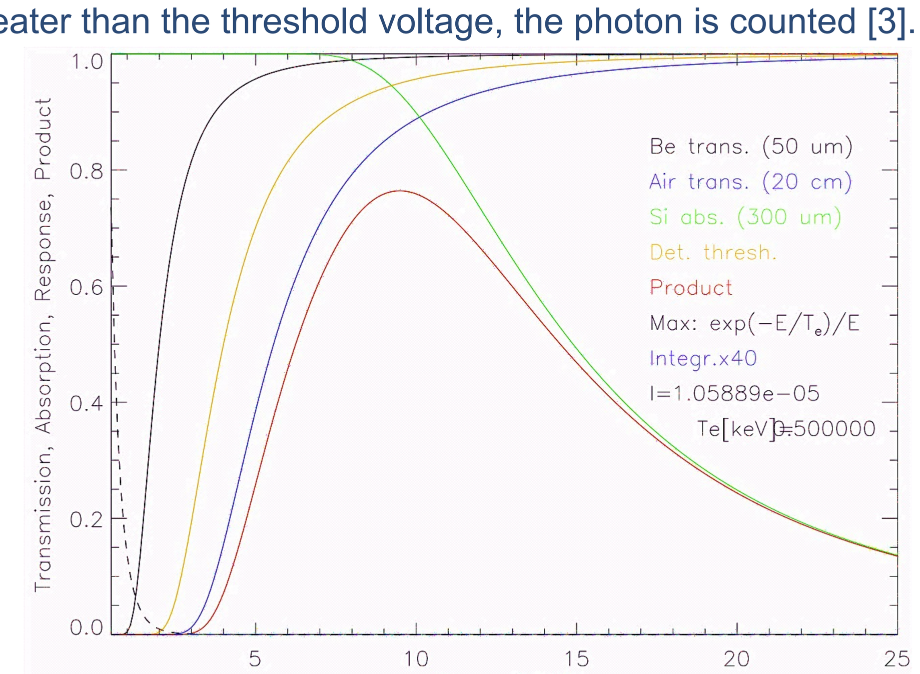

The energy thresholds are set to give the picture of the rate of decay of the bremsstrahlung radiation in the line free region of the plasma [2].

To isolate the continuum emissions, we are concerned with picking an energy window which avoids impurity lines. The most common impurities in C-Mod are Molybdenum from the plasma facing components and Argon (trace amounts) which is used for diagnostic purposes [7, 9]. The energy thresholds are set between 4 eV and 16 keV, at 1 keV intervals, where Mo and Ar are line free.

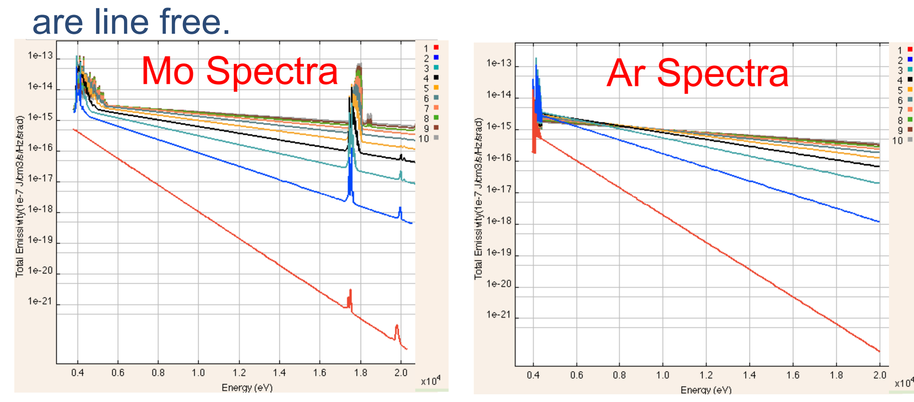

Lines for temperatures ranging from 1 keV to 10 keV show that the emissions for Ar and Mo are line free in the energy region of interests [11].

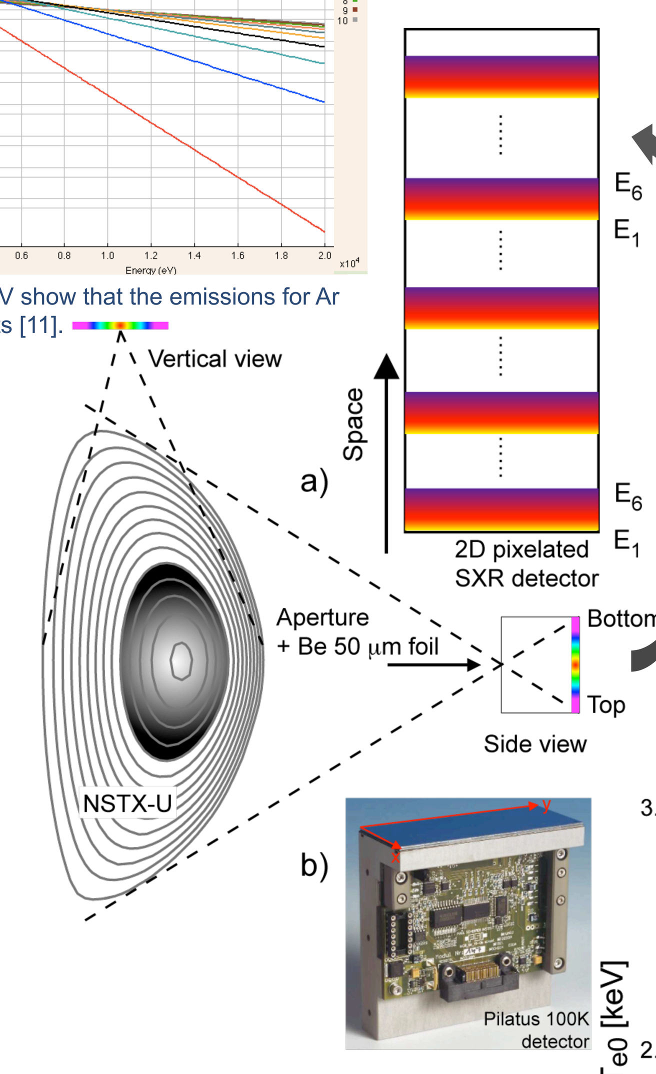

Temperature profiles are given by spacing and repeating the different energy thresholds along the height of the detector [7, 8]. Different channels of the detector report the emissions from different parts of the plasma.

Measurements are integrated along the line of sight of the detector such that the emissivity is a report of the average conditions along that line. This reports the inner plasma conditions in cases where density and temperature drop off rapidly at the plasma edge.

Count Measurements from X-Ray Detector

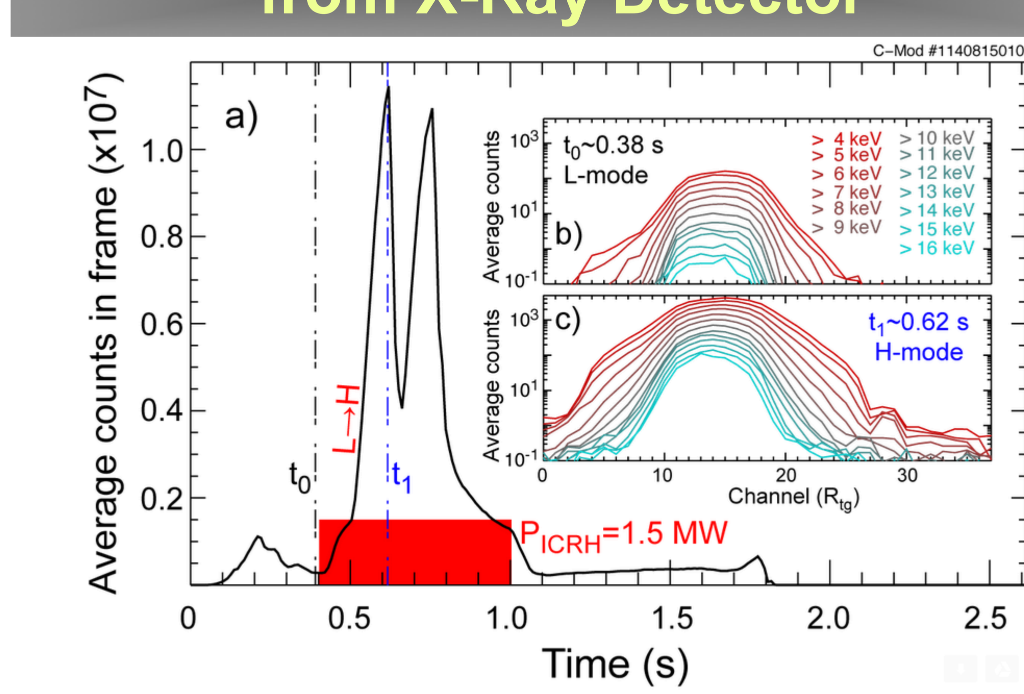

Brightness intensities are measured (line integrated) on each channel (inset plots b and c) for the duration of the plasma shot at C-Mod [7].

The decay of intensities as a function of energy can be resolved for each "energy channel" of the detectors.

Primary times of interest are before and during the ion cyclotron resonance heating (ICRH, highlighted in red).

We calculate electron temperature before, during and after transitions between low (L) and high (H) confinement modes present.

Determining Electron Temperatures from X-Ray Counts

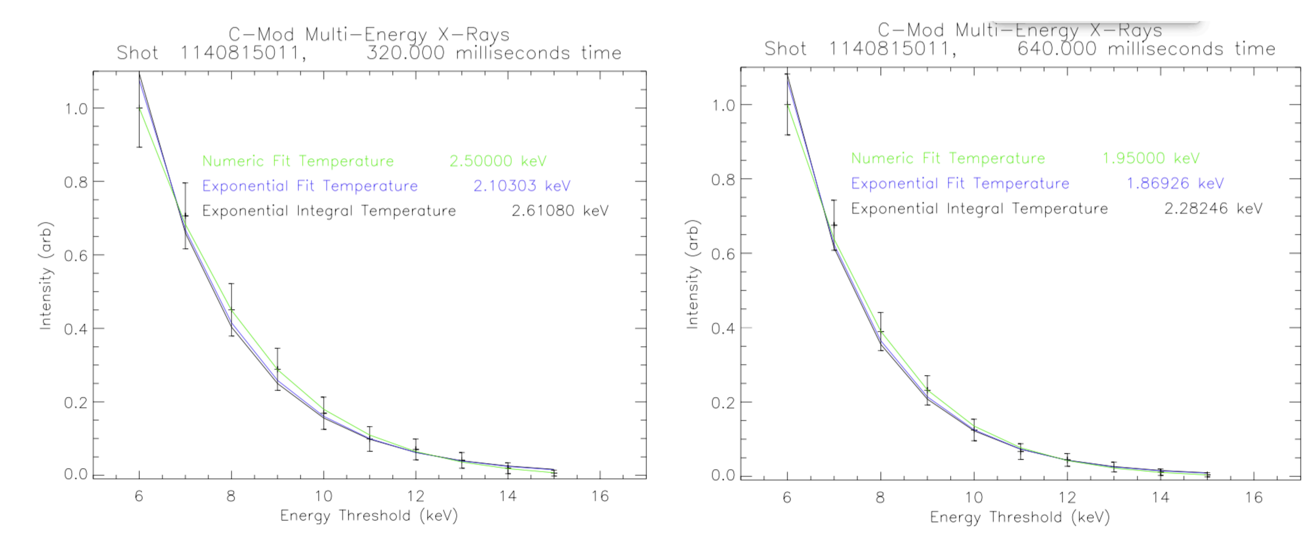

The above fits focus on the central region of the plasma and the channels where x-ray counts are maximum.

$$I_{x-ray_{thresh}} \propto \int_0^\infty \frac{exp(-E/T_e)}{E} Tr^{Be} Tr^{Air} Ab^{Si} S_{Detector} dE$$

Each curve represents three different potential solutions to intensity measurements; an exponential, exponential integral, and a numerical simulation. The parameters of the fit determine electron temperature

$$I_{x-ray_{thresh}} \propto E_1(-E/T_e) \qquad I_{x-ray_{thresh}} \propto exp(-E/T_e)$$

The exponential integral and exponential solutions do not include the physics of the transmission or the electric response of the detector and thus do not fit the data as well but still provide an interesting comparison to the numerical solution of the integral.

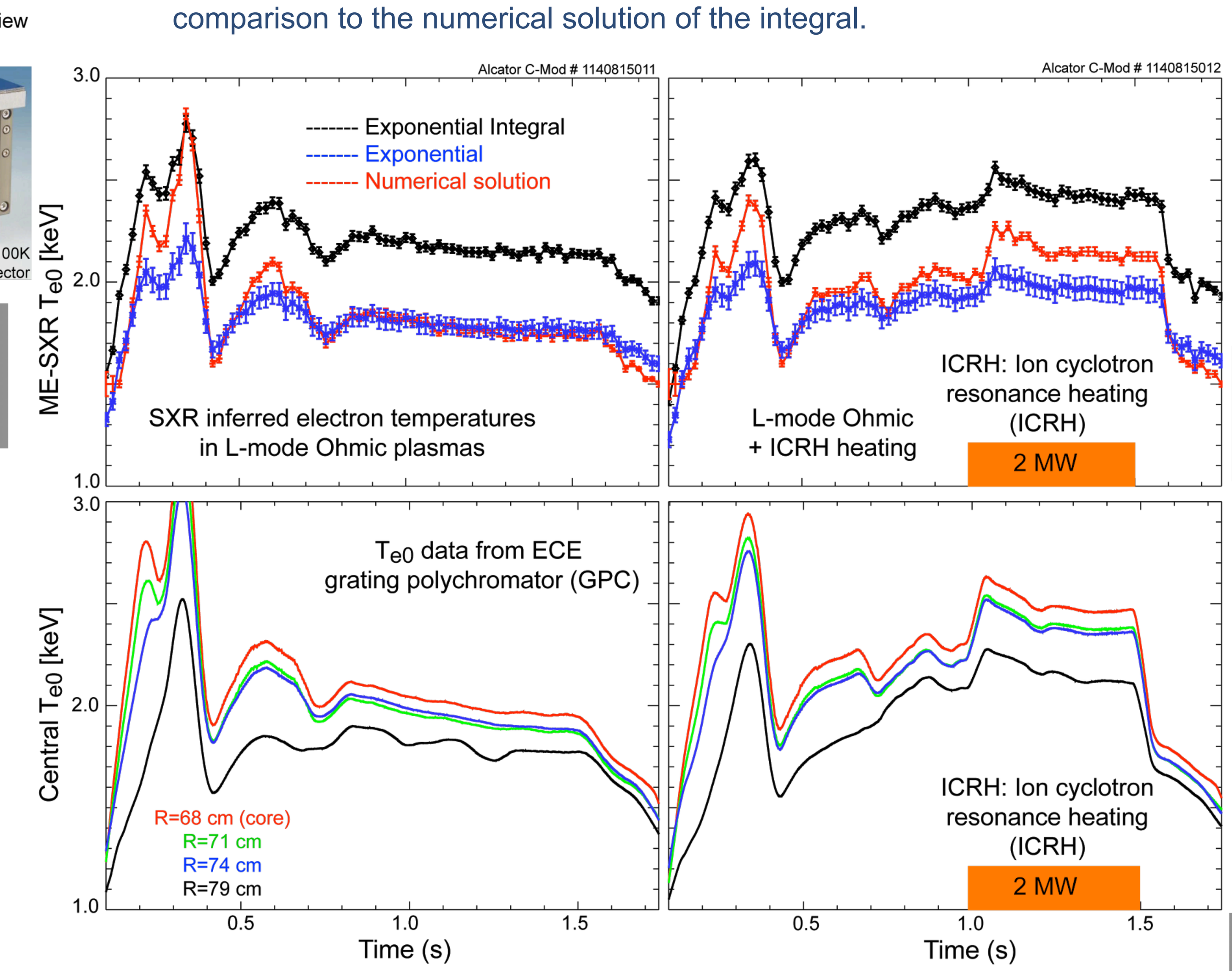

$$\frac{I_{x-ray_{thresh}} - I_{x-ray_{thresh_{max}}}}{I_{x-ray_{thresh_{min}}} - I_{x-ray_{thresh_{max}}}} \propto \int_0^\infty \frac{exp(-E/T_e)}{E} Tr^{Be} Tr^{Air} Ab^{Si} S_{Detector} dE$$

The results for electron temperature are plotted against each other over the duration of the shot.

Intensities were recorded with 20 ms exposure times to ensure counts high enough at all energies to be statistically relevant.

The parameter determining the rate of decay of x-ray intensity determines the electron temperature for each fit.

The numeric fit captures the physics of the x-ray transmission as photons reach the detector. The numeric fit temperatures are compared against ECE and TS.

Future Work

Our line of sight integral measurements can be inverted to find the emissivity at each flux surface.

E_j is the emissivity of each flux surface which multiplied by each surfaces length section L_{ij} and summed gives the total line of sight intensity, B_i which is measured by the detector, by inverting we find the emissivity of each flux surface, E_j.

$$B_i = \Sigma_j L_{ij} E_j, \qquad E_i = \Sigma_j L_{ji}^{-1} B_i$$

The emissivity ratios of each surface gives us an electron temperature profile of the plasma.

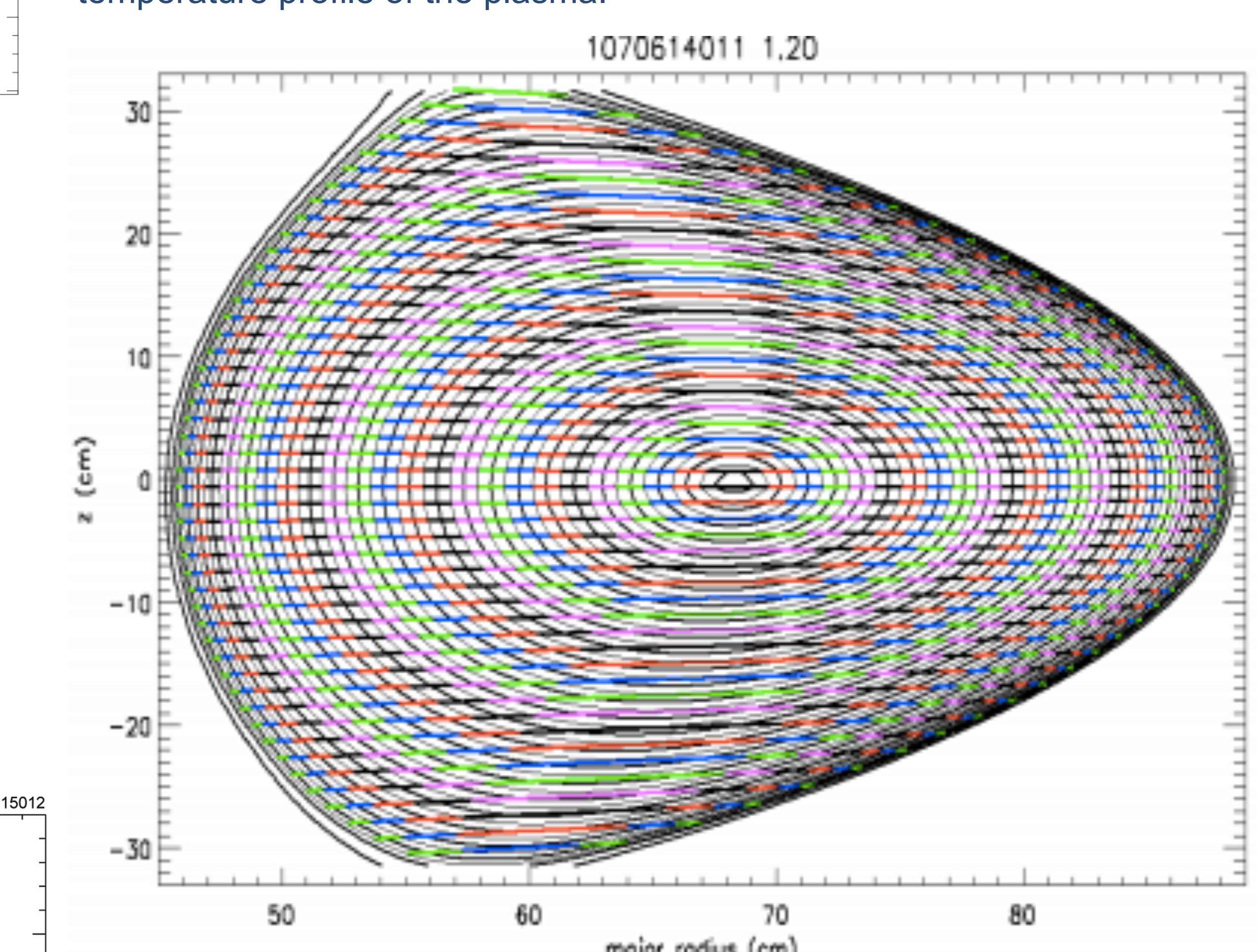

Impurity lines and emissivity profiles could also be used to map transport by generating ion distribution profiles with the same inversion techniques used here for finding electron temperatures.

Conclusions

State of the art x-ray detection can be used to infer the central electron temperatures without the diagnostic footprint, complications and cost of ECE and TS systems.

Adequate spatial and temporal resolution can be obtained.

The Bremsstrahlung emission can be used as long as line free regions of the spectrum can be found and detected.

This technique will be explored in tokamaks with W walls.

Radiation hardened detectors and shielding will be needed.

References

[1] M. Diesso, K. W. Hill, *et al*, Rev. Sci. Instruments, **59**, 08, p.1760, (1986).
[2] L. Delgado-Aparicio, D.Stutman, *et al*, Journal of Applied Physics **102**, 073304 (2007).
[3] Pilatus Detection Systems User Manual. Version **1.3** Dectris. (2007).
[4] L.F. Delgado-Aparicio, D.Stutman, Plasma Phys. Control. Fusion. **49**, p.1245–1257 (2007).
[5] E. Wang, P. Beiersdorfer, *et al*, Rev. Sci. Instrum. **83**, 10E139 (2012)
[6] L. Delgado-Aparicio, K. Tritz, *et al*, Rev. Sci. Instrums. **81**, 10E303 (2010)
[7] L. Delgado-Aparicio, DOE/Office of Science Program Office: Office of Fusion Energy Sciences (2014).
[8] L.F. Delgado-Aparicio, *et al*, PPPL Report (2014).
[9] K. Brau, S. von Goeler, *et al*, Physical Review. **22**, 6, 2769(1980).
[10] N. A. Pablant, L. Delgado-Aparicio, et al., Rev. Sci. Instrum. **83**, 10E526 (2012).
[11] *FLYCHK: Generalized population kinetics and spectral model for rapid spectroscopic analysis for all elements*, H.-K. Chung, M.H. Chen, W.L. Morgan, Yu. Ralchenko, and R.W. Lee, *High Energy Density Physics* v.**1**, p.3 (2005)

Acknowledgements

This work was supported by the US DOE Contract No.DE-AC02-09CH11466 and the DoE Summer Undergraduate Laboratory Internship (SULI) program.